Theoretical Study on Pt Particle Adsorbate Bonding: Influence of Support Ionicity and Implications for Catalysis

Michiel K. Oudenhuijzen,[†,‡] Jeroen A. van Bokhoven,[§] David E. Ramaker,[||] and Diederik C. Koningsberger*[,†]

Department of Inorganic Chemistry and Catalysis, Debye Institute, Utrecht University, P.O. Box 80083, 3508 TB Utrecht, The Netherlands. Chemistry Department, George Washington University, Washington, D.C. 20052

Received: June 28, 2004; In Final Form: September 16, 2004

The influence of the support ionicity on the adsorption of H, CH_x ($x = 2, 3$), and O on supported Pt particles is investigated using density functional theory (DFT). The DFT calculations reveal that the importance of the 6s,p states for the Pt adsorbate bonding increases in the order Pt−O < Pt−CH_2 < Pt−CH_3 < Pt−H. Both the Pt−H and Pt−O bond strengths are strongly affected by changes in the support ionicity whereas the difference for the Pt−CH_x bond strength is much smaller. The Pt−H bond strength is higher for ionic supports, whereas the Pt−O bond strength is higher for acidic or more covalent supports. These bond strength changes occur because the support ionicity has a large impact on both the Pt 6s,p and 5d states. On ionic supports with electron rich oxygen atoms, the 6s,p states are pushed toward the surface of a metal cluster where it can participate in H bonding, whereas on supports with electron poor oxygen atoms (existing in acidic supports or for supports with more covalent cations) the 6s,p states are attracted toward the metal−support interface. The Pt 5d states shift to lower binding energy (lower ionization potential) on ionic supports, where it bonds less effectively with the O adsorbate. These findings indicate that the hydrogen and oxygen coverage on Pt particles are strongly determined by the ionicity and acid/base properties of the support and therefore may be the most important for producing changes in the reactivity of Pt wit support ionicity in various hydrogenolysis, hydrogenation, and oxidation reactions.

Introduction

Supported noble metal catalysts are widely used in commercially important reactions, including hydrogenation, naphtha reforming, and isomerization reactions, and in electrocatalysis redox reactions involving O_2 and H_2 such as that taking place in a fuel cell.[1] Dalla Batta and Boudart made the first report of enhanced reaction rates with specific supports.[2] Since then, it has been well established that the nature of the support influences the rate of hydrogenation and hydrogenolysis reactions on catalytically active metal particles.[3−10] For example, in the conversion of neopentane ($C-(CH_3)_4$), it has been observed that the rate of hydrogenolysis is several orders of magnitude higher when Pt particles are supported on an acidic support compared to a basic support. In addition, the inhibition by hydrogen of the hydrogenolysis of alkanes is much stronger for basic supports: the order in H_2 ranges from −2.5 (basic support) to −1.5 (acidic).[10−13]

Although the effect of the support on the catalytic properties of the supported metal particles has been well established, at least for reactions involving H, the nature of this metal−support interaction has been the subject of much debate. Explanations have involved the formation of metal−proton adducts on Brønsted acidic supports,[5,14] electron transfer between support and particle,[4,15,16] the polarization of the metal particle by nearby cations,[17] and a change in the ionization potential of the metal, due to a shift in the d-band density of states.[8,9,18,19]

Work by our group revealed that the nature of the metal support interaction involves a change in the electronic properties of the metal cluster, induced by and correlated to the electron richness of the support oxygen atoms.[8,9,18] This oxygen electron richness is determined primarily by the ionic character of the cations in the oxide support; with electron rich oxygens existing in basic supports with alkaline cations, and electron poor oxygens existing in acidic supports with protons or other more covalent cations. X-ray absorption fine structure experiments (L_2 and L_3 near edge structure and Atomic XAFS) and density functional theory (DFT) calculations on supported Pt clusters revealed that the support influences the electronic properties of a metal particle in at least three separate ways: (i) the complete Pt density of states (DOS) shifts to higher energy (lower binding energy) with increasing electron richness of the support oxygen atoms,[8,9] (ii) the location of the 6s,p bonding orbital (IBO: interstitial bonding orbital[20]) moves from the metal−support interface to the surface of the Pt particles with increasing electron richness of the support oxygen atoms,[18] and (iii) the insulator to metal transition with increasing cluster size is shifted to lower particle sizes on basic supports.[21]

The change in electronic structure of the Pt particles induced by the support ionicity and acid/base properties will affect the bonding of adsorbates on the Pt surface; however, it is not clear which of the above-mentioned changes in electronic structure play a dominant role in the bonding of adsorbates. Recent

* Corresponding author. Tel: +31302573400. E-mail: d.c.koningsberger@chem.uu.nl.

[†] Utrecht University.

[‡] Present address: GE Plastic Europe, P.O. Box 117, 4600 AC Bergen op Zoom, The Netherlands.

[§] Present address: Lab. für Technische Chemie, ETH Hoenggerberg/HCI E115, CH-8093 Zürich, Schweiz.

[||] George Washington University.

10.1021/jp047193n CCC: $27.50
Published on Web 12/02/2004

theoretical calculations reported in the literature are mostly performed on slabs with periodic boundary conditions, or on relatively small clusters chosen to model flat Pt(111) surfaces (see review of these calculations in ref 23). In contrast, our group[10,22,23] performed density functional calculations using the ADF code on a model $Pt_4/(X_2O_3)$ cluster, where the X_2O groups mimic the support (X = F, covalent; X = H, neutral; X = Na, ionic) to investigate the influence of the electron richness of the support oxygens on the electronic structure of small Pt particles. The calculations show that the Pt−H bond strength is higher for Pt particles on ionic supports. The atop position for hydrogen adsorbed on Pt is preferred only at very low H coverage and low Pt coordination (cluster corners).[22,24] Increasing the hydrogen coverage forces this atop H to move to an *n*-fold site, to reduce lateral interactions. The calculations show that the adsorption energy in the *n*-fold sites existing at high hydrogen coverage increases on the ionic (basic) supports, implying that the fraction of strongly bonded hydrogen is larger in ionic (basic) supports. This knowledge together with information on the dominant hydrogen absorption sites (atop or *n*-fold) obtained from Pt L_3 X-ray absorption near edge data (XANES), was used to analyze previously reported neopentane hydrogenolysis kinetic data.[10] The results from that analysis provided a basic understanding of the metal−support interaction for hydrogenolysis reactions of alkanes catalyzed by Pt particles on supports with different ionicity and acid/base properties. At a fundamental level, the support alters the equilibrium thermodynamic coverage of H. This influences the bonding of the neopentane to the surface, thereby changing the "apparent" activation energy for the reaction.

The effects of the support on the adsorption of oxygen are in the opposite direction to that found for hydrogen.[23] The Pt−O bond strength is higher for Pt on supports with a lower electron richness (covalent or acidic). The oxygen adsorption site also depends on the support properties. Oxygen is adsorbed in a 3-fold hcp and/or subsurface Pt site on supports with low electron richness of the support oxygen, whereas on ionic supports the 2-fold (bridge) sites are preferred.[25] These bond strength changes could be related to the increase in energy position (higher binding energy) of the Pt 5d orbitals with covalent or acidic supports. This shift to higher binding energy leads to a more covalent character (stronger bond) in the Pt−O interaction.

It remains unclear how the bonding of hydrocarbons is affected by changes in the electronic properties of supported metal clusters. It seems obvious that the changes in the DOS within a supported Pt particle as a function of the support ionicity and acid/base properties will affect the chemisorption of CH_x and other hydrocarbons on the surface as well, but will they track in the direction of H or O bonding. The reported data in the literature regarding the adsorption of CH_x on metals mainly focus on Pt(111) flat surfaces.[20,26−28] However, the flat surfaces areas are very small in the case of highly dispersed metal particles, because these particles mainly consist of edge and step sites. Theoretical work has suggested that the metal d states are more important for chemisorbed CH_x fragments.[20,26−28]

In this paper the influence of the support ionicity on the chemisorption of O, CH_x, and H is compared with the help of density functional calculations using the ADF package.[29] CH_3 and CH_2 adsorbates are modeled on a $Pt_4/(X_2O)_3$ cluster (see Figure 1) exactly similar to our previously reported calculations on H and O. Because it is computationally expensive (although possible) to simulate a complete support matrix, the Pt_4 clusters in this work are placed on three X_2O molecules to mimic the support, where the O atoms mimic similar oxygen atoms of the support. The change in O−Si (Al) ionic character, which alters the O support atoms in "real" supports from being electron rich (ionic, basic supports) to electron poor (covalent, acidic supports) is simulated in the cluster by varying the nature of the X atom. F_2O (F is very electronegative, therefore giving an electron poor oxygen atom) represents an acidic support whereas Na_2O (Na is less electronegative than oxygen, thus giving electron rich oxygen atoms) mimics a basic support. It was shown earlier[10,22,23] that this simple model of cluster plus support reproduces the electronic structure of the Pt clusters and the changes with support ionicity quite well. However, with six X atoms near the Pt_4, the $Pt_4/(X_2O)_3$ cluster perhaps models extremely acidic and basic supports and may not be modeling all aspects of the support accurately; such as the local field in an ionic oxide. The theoretical results will show that the support ionicity has a very strong influence on the adsorption of H and O, whereas the effect of the support on CH_3 and CH_2 adsorption is much smaller. The shift in location of the IBO within the Pt particle and the position in energy of the 5d orbitals induced by the support ionicity are the most critical factors in altering the Pt−H and Pt−O adsorption energy, respectively. The implications of these results for catalysis will be discussed.

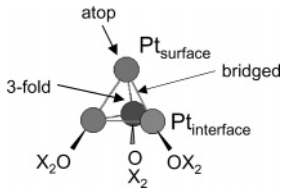

Figure 1. Pt_4/X_2O cluster with three different adsorption sites.

Computational Methods

The DFT calculations reported here have been performed using the Amsterdam Density Functional Package ADF.[29] This package uses the Kohn−Sham approach to the density-functional theory. Slater-type orbitals are used to represent the atomic orbitals. All basis sets consist of triple-ζ quality, extended with two polarization functions. The density functional was calculated using the Vosko−Wilk−Nussair approximation of the local density approximation (LDA), and using the Becke gradient correction[30] and Perdew correlation term[31] for the generalized gradient approximation (GGA). To enhance computational efficiency, several atomic core shells of the Pt atoms were frozen up to and including the Pt 4d level. Relativistic effects were accounted for using the ZORA approximation.[32,33] The geometry optimizations that were performed were carried out in the spin-restricted mode including scalar relativistic effects, thereby excluding spin−orbit effects. This level of accuracy has been reported to agree well with experimental data.[34] The numerical integration precision applied was set to 5.5 significant digits. The applied criteria for the geometry optimization were 1×10^{-3} hartree for the changes in energy, 1×10^{-4} hartree/Å for changes in the energy gradients and 1×10^{-2} Å for changes in the Cartesian coordinates.

The clusters that were investigated consist of a Pt_4 tetrahedron supported by three X_2O molecules, with X = Na or F. The global geometry is shown in Figure 1. In this small Pt_4 cluster all four Pt atoms are at the surface of the cluster; however, only the apical Pt atom is designated $Pt_{surface}$, because in the model cluster this Pt atom is involved with bonding to the adsorbates in all cases. In contrast, the Pt atoms labeled $Pt_{interface}$ are in direct contact with the support, and bond with the asorbate only in the bridged, and fcc adsorbate binding sites. The geometry

TABLE 1: Heat of Adsorption (E_{ads}) and Intrinsic Bond Energy (E_{int}) for the Adsorption of H_2 and CH_n in the Atop, Bridged (br), and 3-Fold Hollow Site (3-f) on Pt_4/F_2O or Pt_4/Na_2O

		E_{ads} (kJ/mol)		E_{int} (kJ/mol)	
adsorbate		Pt_4/F_2O	Pt_4/Na_2O	Pt_4/F_2O	Pt_4/Na_2O
H[a] (22)	atop	−106.0	−175.2	−375.8	−410.4
	br	+105.4	−14.8	−270.1	−330.2
	3-f		unstable[b]		
CH_3	atop	−59.7	−110.1	−303.8	−319.5
	br		unstable[b]		
	3-f		unstable[b]		
CH_2	atop	+1.6	−86.7	−553.4	−572.5
	br	−49.6	−105.7	−604.6	−591.5
	3-f	+23.2	unstable[b]	−531.8	unstable[b]
O (23)	br			−545	−383

[a] The adsorption energy E_{ads} for H_2 is in kJ/mol of H_2; the intrinsic energy E_{int} is in kJ/mol of H. [b] The adsorbed fragment drifted to the most stable position during the geometry optimization.

of the clean Pt_4/X_2O was optimized within the boundaries of C_{3v} symmetry. CH_3 or CH_2 fragments were placed in the atop, bridged or 3-fold sites (see Figure 1). The Pt_4 cluster with adsorbate was allowed to relax its geometry within the limits of C_s symmetry; however, the coordinates of the X_2O molecules were fixed to represent the rigid nature of a real support.

The bond energy is calculated in two ways. The "heat of adsorption", E_{ads}, reflects the decomposition of the gas-phase molecule into fragments followed by adsorption of these fragments onto the Pt cluster. The gas-phase molecule was either H_2 or CH_4. Thus, E_{ads} for H_2 is calculated by taking the difference in the total energy of Pt_4-H/X_2O and $H_2 + Pt_4/X_2O$:

$$E_{ads,H_2} = 2E_{Pt_4-H/X_2O} - 2E_{Pt_4/X_2O} - E_{H_2} \quad (1)$$

The total energy of a cluster was determined relative to the atomic reference energies according to Baerends et al.[35] In calculating the adsorption energy of CH_n it was assumed that the hydrogen fragment adsorbs on a clean cluster, and thus the adsorption energy E_{ads} is given by:

$$E_{ads,CH_n} = E_{Pt_4-CH_n/X_2O} + (4-n)E_{Pt_4-H/X_2O} - (5-n)E_{Pt_4/X_2O} - E_{CH_4} \quad (2)$$

The "intrinsic bond energy" reflects the energy required to remove a fragment adsorbed on the Pt_4 cluster to the gas phase. It is given for hydrogen bonded on Pt_4 by

$$E_{int,H} = E_{Pt_4-H/X_2O} - E_H - E_{Pt_4/X_2O} \quad (3)$$

and for a CH_n fragment bonded on Pt_4:

$$E_{int,CH_n} = E_{Pt_4-CH_n/X_2O} - E_{CH_n} - E_{Pt_4/X_2O} \quad (CH_n \text{ bonding}) \quad (4)$$

Results

Hydrogen Adsorption. Although the calculations for H on the model cluster utilized in this work have been reported previously, the heats of adsorption, E_{ads}, and intrinsic bond energies E_{int} for Pt−H are given here in Table 1. The optimized geometries are given in Figure 2 for completeness. Regardless of the support (Na_2O vs F_2O), when starting in the 3-fold hollow site, the hydrogen drifts to the atop site after geometry optimization. Moreover, a single hydrogen in the atop site is much more stable than in the bridged site (Table 1). Also, E_{ads} for this single atop H atom is 70 kJ/(mol H_2) more exothermic for Pt_4/Na_2O than for Pt_4/F_2O. Analogous to the heat of adsorption, the intrinsic bond strength is increased by 35 kJ/(mol H) for the basic support.

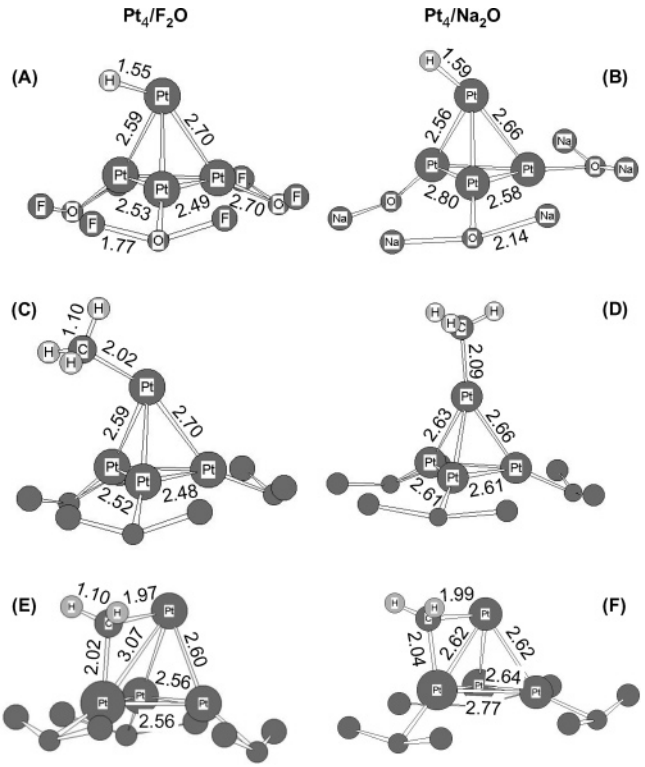

Figure 2. Optimized geometries of a Pt_4 cluster. Hydrogen adsorbed in the atop position: (A) F_2O and (B) Na_2O support. CH_3 adsorbed atop: (C) F_2O and (D) Na_2O support. CH_2 adsorbed in the bridged position: (E) F_2O and (F) Na_2O support. The C−H bond length was not affected by the support, the Pt−O and O−X bond lengths were unaffected by the adsorbate. The bond lengths are given in Å.

The hydrogen in the atop site is found to be tilted toward the interface, and this tilt is largest in the case of the Pt_4/F_2O: compare Figure 2A with B. The Pt−H bond length is 1.55 Å for adsorption in the atop position on the Pt_4/F_2O cluster, with Pt−Pt bond lengths varying from 2.49 to 2.59 Å. For Pt_4/Na_2O, the Pt−H bond length is 1.59 Å, and the Pt−Pt bond lengths range from 2.56 to 2.59 Å.

The gross population density of states (GPDOS) for the H and $Pt_{surface}$ atoms for the Pt_4/F_2O and Pt_4/Na_2O clusters are shown in Figures 3 and 4, respectively. Several observations can be made: The H 1s state around −12 eV is split into multiple peaks, with maxima aligning with peaks in the Pt 6s,p DOS. The Pt 5d band also has significant intensity and overlaps with the maxima in the H 1s DOS, suggesting that 5d also participates in the bonding. Above the Fermi level, the H 1s−Pt 6s,p antibonding state (AS) is clearly visible. Compared with the acidic F_2O support, the H 1s also overlaps similarly with the Pt 6s,p and Pt 5d states on the Na_2O support, but now much more with the Pt 6p. Indeed, the significant increase of 6s,p contribution overlapping with the H 1s around −4 and −9 eV appears to be the major difference between the F_2O and Na_2O supports. Moreover, there are clearly more Pt 6sp states below the Fermi level in the Na_2O case.

CH_3 Adsorption. The most favorable adsorption site for a single CH_3 on the supported Pt_4 cluster is the atop position. If CH_3 was placed in another adsorption site initially, it drifted to the atop position during the geometry optimization. The optimized geometries for CH_3 adsorbed on the Pt_4/F_2O and $Pt_4/$

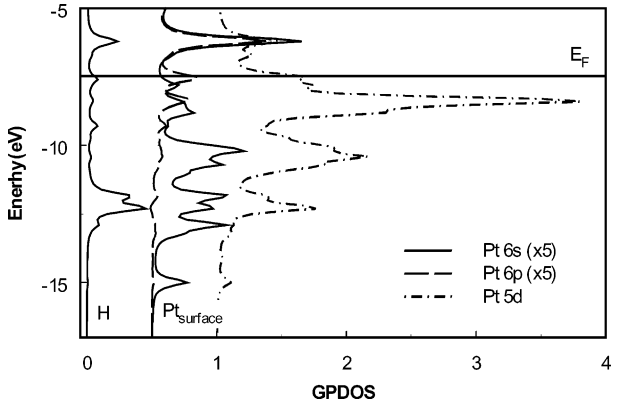

Figure 3. H 1s GPDOS and the surface Pt atom 5d,6s,p GPDOS for hydrogen adsorbed in the atop position on a Pt_4/F_2O cluster. The Pt 6s and 6p GPDOS is magnified by a factor of 5. E_F is the Fermi level.

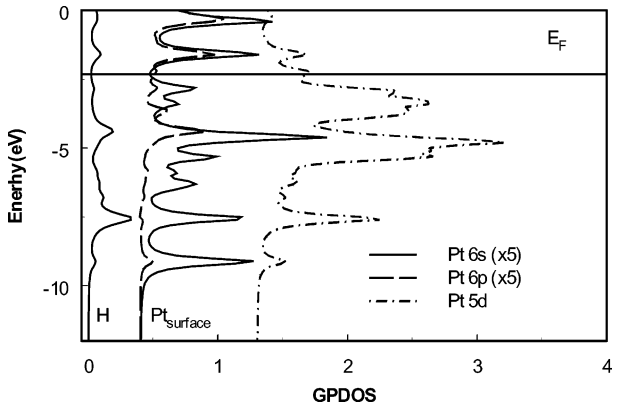

Figure 4. H 1s GPDOS and the surface Pt atom 5d,6s,p GPDOS for hydrogen adsorbed in the atop position on a Pt_4/Na_2O cluster. The Pt 6s and 6p GPDOS is magnified by a factor of 5. E_F is the Fermi level.

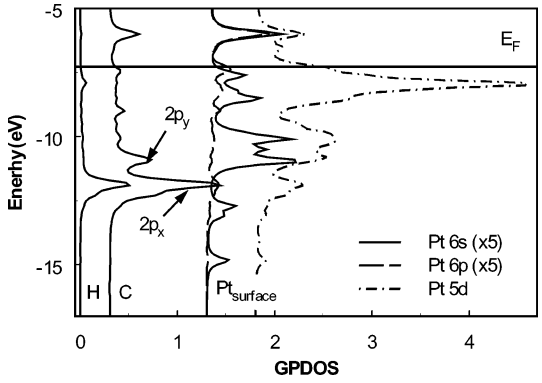

Figure 5. H 1s GPDOS, C 2s,2p GPDOS and the surface Pt atom 5d,6s,p GPDOS for CH_3 adsorbed in the atop position on a Pt_4/F_2O cluster. The Pt 6s and 6p GPDOS is magnified by a factor of 5. E_F is the Fermi level.

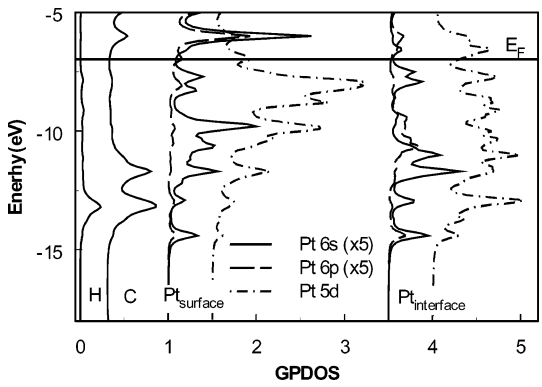

Figure 6. H 1s GPDOS, C 2s,p GPDOS and the surface and interface Pt atom 5d,6s,p GPDOS for CH_2 adsorbed in the bridged position on a Pt_4/F_2O cluster. The Pt 6s and 6p GPDOS is magnified by a factor of 5. E_F is the Fermi level.

Na_2O cluster are shown in Figure 2C,D. The Pt−C bond length for the Pt_4/F_2O (and Pt_4/Na_2O) cluster is 2.02 Å (2.09 Å) and the Pt−Pt bond lengths range between 2.48 and 2.70 Å (2.61 and 2.66 Å). The CH_3 adsorbate is tilted toward the interface with the F_2O support, but nearly perfectly in the atop geometry for the Na_2O support.

The intrinsic bond energy E_{int} for Pt−CH_3 is smaller for the acidic support (Table 1), just as was observed for the Pt−H bond; however, the difference is much smaller for CH_3: 16 kJ/(mol CH_3) vs 35 kJ/(mol H). The heat of adsorption for CH_3 is 50 kJ/mol smaller in the case of an acidic support compared to a basic support.

The GPDOS for CH_3 adsorbed in the atop position on the Pt_4/F_2O cluster is shown in Figure 5. Because no extra information is obtained from the results for the Pt_4/Na_2O cluster, these results are omitted. For the Pt_4/F_2O cluster, the DOS show maxima at approximately −12 eV for both the H 1s and C 2s,p states. These maxima represent the C−H bond involving the C $2p_z$ orbital. This C−H bonding orbital is degenerate with some Pt 5d states, indicating that some mixing between those orbitals occurs. The overlap between the C 2s and H 1s orbital is located at lower energy and is not shown in Figure 5. At ∼−11 eV, a second, smaller peak in the C 2p DOS is visible, corresponding to a peak in the Pt 6s,p states. The H 1s shows no intensity at that energy, suggesting that this is primarily the Pt−C bond. Therefore the Pt−C has significant 6s and 5d character. Just above the Fermi level another maximum in the C 2p and Pt 6s,p states is visible, showing the antibonding state.

CH_2 Adsorption. The favored adsorption site for the CH_2 fragment is the bridged site for both supports. The optimized geometries are shown in Figure 2E,F. The two hydrogen atoms are eclipsed with respect to the two Pt atoms bonded to the carbon. In other words, CH_2 shows a tetrahedral coordination together with the two Pt atoms. The $Pt_{interface}$−C bond lengths are 2.02 and 2.04 Å and the $Pt_{surface}$−C are 1.97 and 1.99 Å for Pt_4/F_2O and Pt_4/Na_2O, respectively. The Pt−Pt bond length between the 2 Pt atoms in the cluster that bond to the CH_2 decreases from 3.07 to 2.62 Å for Pt_4/F_2O and Pt_4/Na_2O, respectively.

The other adsorption positions, the 3-fold hollow site and the atop site, are less stable by 50−70 kJ/mol (Table 1). If CH_2 is initially placed in the 3-fold site for the Pt_4/Na_2O cluster, it drifts toward the atop position during the geometry optimization. Due to symmetry restrictions in this calculation (the symmetry is C_s), the CH_2 fragment cannot move to the bridged site.

The intrinsic bond energy of CH_2 in the bridged position is lower by 13 kJ/mol in the case of the acidic F_2O support (−605 kJ/mol vs −592 kJ/mol). This is the reverse order to that found for the adsorption of H and CH_3, which were adsorbed more strongly on the basic supported Pt_4 cluster. In contrast, the heat of adsorption, which includes the adsorption of 2 hydrogen atoms, is lowest in the case of the basic support (−105.7 kJ/mol compared to −49.6 kJ/mol).

Figure 6 shows the GPDOS for the CH_2 adsorbed on a Pt_4/F_2O cluster in the bridged position. The results for the Pt_4/Na_2O cluster are omitted here because no critical information is

obtained from these DOS. Only the H 1s, C 2s,p and Pt 5d 6s,p DOS of the Pt atoms attached to the CH_2 are shown (Figure 6). At ∼−13 eV the C 2p and H 1s DOS show simultaneously a maximum, representing the C−H bond. The Pt states peak at a little higher energy, indicating that the mixing between the C−H bond and Pt states is limited. At −12 eV, the C 2s,p states show a second maximum in the DOS, this is essentially the Pt−C bond. The Pt 5d and 6s,p DOS for both the surface and the interface atoms peak at the same position. Compared to CH_3 adsorption (Figure 5), the relative intensity of the Pt 6s,p states is decreased significantly in the primary Pt−C bond orbital. Just above the Fermi level at −6 eV, the C 2p and Pt 6s,p states reveal an antibonding state. Note the large Pt_{surf} 6s,p contribution in this antibonding orbital compared to the atop CH_3 case, reflecting the decreased importance of 6sp bonding in the bridged CH_2 case.

Discussion

Hydrogen Adsorption. The Pt−H bond lengths with H in the atop position (1.56 and 1.59 Å for the F_2O and Na_2O supports, respectively) are in good agreement with the value of 1.57 Å reported by Papoian et al.[28] The Pt−Pt bond lengths, which are between 2.49 and 2.59 Å, are low compared to the bulk value of 2.77 Å. However, it is well-known that due to the increasing dehybridization of the Pt valence orbitals for decreasing Pt particle sizes the Pt−Pt bond strength increases and consequently the Pt−Pt coordination distance decreases for small clusters.[20,36] Thus, our calculations clearly reproduce the geometries that have been found in the literature. In general, the favored adsorption position for hydrogen on flat Pt(111) surfaces is the 3-fold site.[28,37] However, for small clusters the first hydrogen that adsorbs is known to go into the atop position.[20,22]

The adsorption energies that are found (−100 to −170 kJ/(mol H_2)) for H adsorption here are larger than is generally found for H/Pt(111) (−35 ±20 kJ/mol).[23,28,34] The much higher adsorption energy for hydrogen on the small model cluster compared to adsorption on Pt(111) surfaces no doubt arises from the low Pt−Pt coordination at such sharp cluster corners where the H is bonded. It also generally agrees with temperature programmed desorption studies that show that all hydrogen desorbs below 300−350 K from Pt(111) surfaces[38−40] whereas hydrogen remains on the surface up to 450 K for stepped edges[38,41,42] or on highly dispersed particles.[25,43]

The origin of the large difference in the adsorption energy for basic and acidic supports lies in the relatively large contribution of Pt 6s,p states to Pt−H bonding, as indicated already in the Introduction. As can be seen in the DOS for the Pt_4/F_2O cluster (Figure 3), the maxima of the H 1s DOS align to a large extent with the Pt 6s,p peaks. This suggests that the bonding of hydrogen to Pt via the Pt 6s,p states is very significant. This has also been reported previously in the literature. Kua and Goddard[20] performed generalized valence bond (GVB) calculations on a series of Pt clusters of variable size and showed that hydrogen binds in part via the so-called "interstitial bonding orbital" (IBO). When bulk Pt is involved, Pt atoms share one IBO in each tetrahedron. In fact, this IBO is the bonding combination of the Pt 6s and 6p orbitals in a Pt_4 tetrahedron. Although others do not use the IBO terminology, it is generally found that the Pt 6s,p states play a significant role in the bonding of H on Pt.[28] The specific symmetry properties of the Pt 6s,p orbitals are very beneficial for Pt−H bonding.

In an earlier paper, it was shown that the location of the IBO within the Pt particle shifts from the metal−support interface to the Pt surface with increasing electron richness of the support oxygen atoms (more basic support).[18] In addition, some antibonding 6s,p states are shifted below the Fermi level and become populated at the cost of the Pt 5d. This can also be seen when the H DOS on Pt_4/F_2O (Figure 3) and Pt_4/Na_2O (Figure 4) are compared. There are clearly more Pt 6s,p states below the Fermi level for Na_2O, and they are at lower energy relative to the Fermi level. These 6s,p states overlap strongly with the H 1s orbital. Effectively, with increasing electron richness, the Pt valence band rehybridizes and obtains more 6s,p character, e.g., from $5d^9 6s^1$ to $5d^{8.8} 6s^{1.2}$.

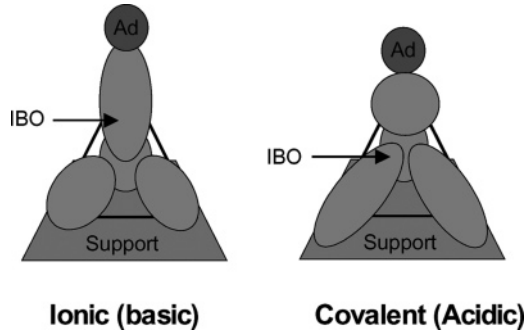

Figure 7. Schematic illustration of the interstitial bond orbital (IBO) inside a tetrahedral Pt_4 cluster on a ionic (basic) and covalent (acidic) support, with one H atom adsorbed in an atop position.

These results show that the changes in the Pt−H bond strength are correlated with changes in the Pt 6s,p states. When the IBO moves toward the metal−support interface, as is the case for the acidic support,[18] it can no longer participate in the Pt−H bond. The IBO is located below the 5d band at −15 eV in the Pt_4/F_2O cluster, and at that energy the H 1s DOS shows no intensity, revealing a lack of bonding between the hydrogen and the IBO. However, on the Na_2O support, the IBO is located at the surface.[18] Therefore, the IBO can participate in the Pt−H bond and this is indeed shown in Figure 4 for the H and $Pt_{surface}$ DOS of Pt_4/Na_2O. In this cluster, the IBO is located at −9 eV, and the H 1s orbital shows a small peak at this energy. Because sp states are mixed with the 5d band to a greater extent on the basic Na_2O support, the altered symmetry of the 5d−6s,p orbital (they become more sp like) improves the overlap with H 1s, and consequently, the Pt−H bond is strengthened.

Figure 7 illustrates the nature of the IBO and how this changes with the acidity of the support on the basis of the ADF results in Figures 3 and 4. Here the IBO is sketched as a combination of Pt 6s,p orbitals overlapping at the center of the tetrahedron. The more Pt 6p character, the more we elongate the orbital on the Pt. Thus on the basic support, the Pt_{surf} 6s,p contribution is significantly elongated, showing a strong overlap with the adsorbate, whereas on the acidic support, the Pt_{int} 6s,p contributions are elongated, showing strong overlap with the support O atoms. Figure 3 (although not showing the DOS on the Pt_{int} atoms) does show small Pt_{surf} 6p DOS just below the Fermi level. This arises because of mixing of the Pt_{surf} and Pt_{int} orbitals, and the P_{int} orbitals are mixing with the O nonbonding orbitals on the support O atoms. Overall, a shifting of the IBO from the surface to the interface occurs with increasing acidity, as illustrated in Figure 7. Because the Pt_{surf}-H bond has a strong Pt 6s,p component, this shift significantly affects the Pt−H bond strength.

The shift of the s,p states toward the interface with the acidic cluster can also explain the remarkable difference in the geometry of the H in the atop position in the Pt_4/Na_2O and Pt_4/F_2O cluster. H is tilted much more toward the interface region

in the case of the acidic F_2O support (Figure 2). Because the Pt 6s,p states are very important in the Pt−H bonding, the hydrogen atom tries to "follow" the metal sp states. Therefore, the Pt 6s,p states not only determine the Pt−H bond energy but also influence the geometry.

The DFT calculations indicate a preference for the atop site at low coverage, especially on these small clusters. So far, atop H has never been seen spectroscopically on Pt, except at very high coverage in an electrochemical cell[39] and on Pt black at low temperatures,[17] but never at temperatures greater than 330 K. Although atop H has been seen via HREELS on Ir(111), it has not been seen on Pt(111) at any coverage or temperature. However, Kua and Goddard[42] have suggested that at very low coverage (below 1/7 monolayer [ML]) H may in fact prefer the atop sites on Pt(111), because it can then maximize its overlap with three interstitial bond orbitals (IBO), although recent ADF results reported by Koper and van Santen[48] do not find this. At coverage above this level, the H clearly prefers the 3-fold fcc sites on Pt(111), where it can maximize its overlap with one IBO, and not have to share with other H. Recently,[22] however, atop hydrogen has been observed for small ($D < 1$ nm) Pt particles dispersed on covalent (acidic) supports. Further, ADF results[22] show that when two or three H atoms are placed on the simple Pt_4 cluster considered here, the H atoms indeed move to the bridged and 3-fold sites, respectively. Thus the preferred adsorption site depends strongly on the H coverage, and the ADF results reported here are not necessarily inconsistent with previously reported theoretical or experimental results.

A point about the zero point energies needs to be made here. The total energy of a cluster was determined relative to the atomic reference energies according to Baerends et al.[35] and the calculations performed were in the spin-restricted mode. A classic example of what can occur in this approximation will become clear from the following. From eqs 1 and 3, the difference $E_{ads,H_2} - 2E_{int,H}$ equals $-E_{H_2} + 2E_H$ with the dissociation energy of the H_2 molecule around 440 kJ/mol.[44] However, the results in Table 1 give this energy difference to be approximately 645 kJ/mol. At equilibrium distance, H_2 is reasonably well approximated in the spin-restricted mode because of the closed shell system, but at the dissociation limit the spin-restricted approximation gives an energy for two separated H atoms that is much too high because of the large ionic components (H^+H^-) forced in this approximation for two separated H atoms.[45] Thus the E_{ads} energies are generally more reliable for comparison with experimental and non-spin-restricted calculations, but both the relative E_{ads} and E_{int} energies are reliable for determining the preferred binding sites.

CH_3 Adsorption. The optimized geometries for CH_3 adsorbed in the atop site show features similar to those of the H adsorbed in the atop position. The Pt−C bond lengths of 2.03 (acidic cluster) and 2.09 Å (basic) are similar to values reported in the literature.[26−28] The favored atop adsorption position is also well-known for the adsorption of CH_3 fragments. CH_n fragments generally tend to maintain the tetrahedral geometry; i.e., CH_3 adsorbs in an atop position, CH_2 in the bridged position, and CH in the 3-fold hollow site.[26−28,46]

We find intrinsic bond energies E_{int} for adsorption of CH_3 and H of −304 kJ/mol (F_2O support) to −320 kJ/mol (Na_2O). This is larger than the values reported in the literature (−200 kJ/mol[46]) for CH_3 adsorption on Pt(111) surfaces. This difference is caused again by the coordinatively unsaturated nature of the Pt atoms in a Pt cluster compared to a flat (111) surface. In addition, the calculations reported here do not fully account for the spin properties, and therefore the true atomic ground state and true bond energy are not calculated. The trends that are observed, however, are not spin-related and can be calculated reliably without using the computationally expensive calculations including spin−orbit effects. Although E_{int} is only lower by 16 kJ/mol for the basic support, the heat of adsorption E_{ads} is lower by 50 kJ/mol. This large drop in E_{ads} reflects the much larger change (35 kJ/mol) in Pt−H bond strength going from acidic to basic supports.

When the DOS for CH_3 vs H adsorbed on Pt_4/F_2O (Figures 5 and 3) are compared, some interesting differences are seen. The C 2p states show some overlap with the Pt 6s,p states, but the degree of overlap is much smaller for Pt−CH_3 than for Pt−H. However, the Pt−CH_3 bond involves more Pt 5d states than the Pt−H bond. This means that the Pt 6s,p states are more important for the Pt−H bonding and that the Pt 5d states are more essential for the chemisorption of CH_3 on Pt.

The Pt 6s and 6p orbitals are very diffuse, whereas the Pt 5d orbitals are more localized with specific geometries. Due to their delocalized nature, the Pt 6s,p states have more interaction with the support and consequently are less affected than the localized Pt 5d states. Because the Pt 6s and p states are more important for chemisorption of H than for CH_3, it can be concluded that the influence of the support is less important for the chemisorption of CH_3.

CH_2 Adsorption. As expected, CH_2 preferentially adsorbs in the bridged position where it can complete the carbon's tetrahedral geometry (Figure 2E,F). The Pt−C bond length of ∼2.00 Å is in agreement with the work of Kua and Goddard,[26,27] but it is much smaller than the 2.3 Å reported by Paul[46] for the adsorption of CH_2 in the bridged position on Pd(111). In the case of the Pt_4/F_2O cluster, the adsorption of CH_2 leads to a large elongation of the Pt−Pt bond length to 3.07 Å between the Pt atoms forming the bridge. This elongation suggests that the CH_2 is adsorbed very strongly, because it weakens the Pt−Pt bond to a large extent. This elongation is not observed for the Pt_4/Na_2O cluster. In agreement with these observations, the intrinsic bond energy E_{int} is more negative (more exothermic) by 13 kJ/mol for the Pt_4/F_2O cluster compared to the Pt_4/Na_2O cluster. However, the heat of adsorption E_{ads} is more negative in the case of the Na_2O support. This again is caused by the larger difference in the Pt−H bond strength, because during the dissociative adsorption of CH_4 as CH_2, $CH_4 \rightarrow CH_2 + 2H$, two hydrogen atoms are adsorbed on the Pt_4 cluster. This means that the dissociative adsorption of CH_4 is more exothermic for adsorption on the Pt_4/Na_2O cluster than it is on the Pt_4/F_2O cluster, although the intrinsic Pt−CH_2 bond strengths are in the reverse order. Clearly, the change in the CH_2 heat of adsorption is governed by the hydrogen intrinsic adsorption energy.

From a comparison of the DOS of CH_2 in the bridged position (Figure 6) with the DOS of CH_3 on the atop position (Figure 5) on the Pt_4/F_2O cluster, it is clear that the CH_2 adsorption involves even less Pt 6s,p states and more Pt 5d states than the CH_3. Therefore, the adsorption of CH_2 is mainly determined by the influence of the support acidity on the d-band. On acidic supports, the d-band is shifted to lower energies, which is beneficial for the overlap of the C 2p and Pt 5d band when CH_2 is adsorbed.

The importance of the Pt 5d states for the bonding of CH_x fragments is in agreement with results reported by Nørskov et al.[47] They show that the adsorption energy correlates with the energy of the d-band center across a transition metal series. The diffuse metal sp states effectively are the same across a transition

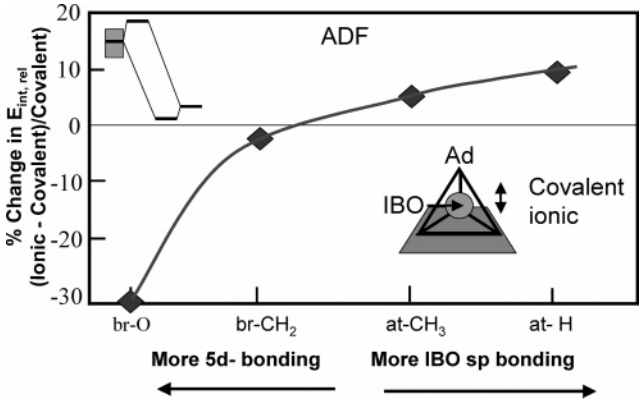

Figure 8. Relative intrinsic bond energy as a function of the type of Pt−adsorbate bonding with the covalent (acid)/ionic (basic) properties of the support as independent parameter. The average E_{int} is set to zero for each adsorbate. The Pt [sp/(sp+d)] ratio determines the support effect.

metal series, and only changes in the d-band are reflected in the adsorption energies.

Oxygen Adsorption. As shown in work previously reported,[23] the Pt 6s,p orbitals are much less significant in the Pt−O bonding compared with Pt−H, so the IBO rearrangement is not primarily responsible for the change in Pt−O bonding with support acidity in this case. Indeed the DFT results in Table 1 confirm that the Pt−O bond strength increases on the acidic $O/Pt_4(F_2O)_3$ cluster compared with the basic cluster $O/Pt_4(Na_2O)_3$ (an increase of nearly 30% compared with a less than 10% decrease for Pt−H; see Table 1). The Figure 8 insert schematically illustrates the decrease in ionic character (increase in covalent character and hence bond strength) of a Pt−O bond with increasing Pt 5d valence band shift to higher binding energy. This schematic is appropriate for a transition metal, an example of the adsorbate/metal bonding in the "two-level" strong adsorption limit.[48]

Influence of the Support Acid/base Properties on the Adsorbate Bonding. When the DOS for adsorption of H, CH_3, and CH_2 in their optimal positions are compared, the importance of the Pt 6s,p states in the bonding increases in the order O < CH_2 < CH_3 < H. The high importance of the metal d orbitals in the M−CH_n bond with highly unsaturated C atoms (e.g., n = 0) was observed earlier[46] and as discussed above, the predominance of Pd d orbital bonding with O is also well-known. The influence of the support acid/base properties on adsorbate bonding appears to be the largest when the adosrbate bonding is dominated by either the Pt 5d or Pt 6s,p. The calculations involving CH_2 and CH_3 adsorbed on $Pt_4(X_2O)_3$ clusters showed relatively small differences in the bonding with a change in X, even though the CH_x fragments also have a strong bonding component with the Pt d orbitals. Indeed the trend in the Pt−C bond strength is in the opposite direction for the atop CH_3 (decrease in Pt−C bonding) versus the bridged CH_2 (increase in Pt−C bonding) fragment with support acidity. It seems clear that the CH_x fragments have significant components of both 5d and 6s,p, and the opposite effects of the 5d valence band shift and 6sp IBO rearrangement on the bonding cancel each other nearly out. The Pt 6s,p/Pt 5d bonding ratio apparently increases in the order O(br) < CH_2(br) < CH_3(atop) < H(atop). Figure 8 shows the change in E_{int} (acid−base/base) relative to that in the acidic support for each of the adsorbates. Further, the relative importance of the Pt 5d vs Pt 6s,p bonding is schematically indicated.

Implications for Catalysis. Figure 8 clearly shows that the support has the most dramatic effect on the H and O adsorption compared to CH_2 and CH_3. This has significant implications for catalysis. It suggests that when changes are seen in the turnover frequency with support ionicity, these changes may result more from changes in the H or O coverage, than from changes in the bond strength of the Pt−hydrocarbon.

As mentioned in the Introduction above, in the conversion of neopentane ($C-(CH_3)_4$), it has been observed that the rate of hydrogenolysis is several orders of magnitude higher when Pt particles are supported on an acidic support compared to a basic support. A detailed analysis of the kinetic data for neopentane hydrogenolysis as reported by us[10] recently showed that the H coverage directly affected the neopentane−Pt bond strength through the Frumkin isotherm and thereby changed the activation energy for the reaction. Preliminary results for the hydrogenation of benzene and other alkenes catalyzed by Pt on supports with different ionicities show that the change in H coverage may be the most responsible for the observed change in reactivity.

The decreasing bond strength of the Pt−O bond with ionicity of the support can also have significant implications for reactions involving O. In the direct methanol fuel cell, CO poisoning of the Pt surface is a severe problem.[49] Pt is often alloyed with another metal such as Ru, to lower the potential for the onset of OH formation from the water. This OH, in the bifunctional mechanism is believed to react with the CO, producing CO_2, which then leaves the surface.[50,51] These results suggest that it is worthwhile to consider changing the support from the usual amorphous carbon at the cathode of the fuel cell. A highly covalent (acidic) support, which according to the results above should decrease the potential for the onset of OH and O formation, should lower the potential when the CO oxidation reaction occurs. This would significantly decrease the CO poisoning and thereby increase the efficiency of the methanol oxidation.

Conclusions

DFT results for CH_x on small supported Pt clusters, along with those reported previously for O and H, show that the importance of the Pt 6s,p states in the chemisorption bond increases in the order O < CH_2 < CH_3 < H. The Pt 5d and 6s,p states are influenced strongly by the support acid/base properties, thereby influencing the bonding of the adsorbates. On covalent (acidic) supports, the sp states are moved toward the metal−support interface, and consequently, the adsorbate bond energies are decreased for CH_3 and H, when Pt 6s,p bonding dominates. However, on ionic (basic) supports the Pt 6s,p states are located at the surface of the Pt cluster and are readily available for the bonding to adsorbates. In contrast, the Pt 5d orbitals dominate for Pt−CH_2 and O adsorbate bonding. In this case the Pt−adsorbate bond is stronger for acidic supports than for basic supports.

These results have significant implications for catalysis. They have already been used to explain the compensation effect and the negative order in the partial pressure of hydrogen found for the hydrogenolysis of neopentane catalyzed by supported Pt particles[10] and have potential for use in designing improved catalysts in the direct methanol fuel cell.

References and Notes

(1) Gates, B. C. *Chem. Rev.* **1995**, *95*, 511−522.

(2) Dalla Betta, R. A., Boudart, M. *Proc. 5th Int. Congr. Catal.* **1973**, 1329−1341.

(3) Homeyer, S. T.; Karpinski, Z.; Sachtler, W. M. H. *J. Catal.* **1990**, *123*, 60−73.

(4) de Mallmann, A.; Barthomeuf, D. *J. Chim. Phys.* **1990**, *87*, 535−538.
(5) Karpinski, Z.; Gandhi, S. N.; Sachtler, W. M. H. *J. Catal.* **1993**, *141*, 337−346.
(6) Xu, Z.; Xiao, F. S.; Purnell, S. K.; Alexeev, O.; Kawi, S.; Deutsch, S. E.; Gates, B. C. *Nature* **1994**, *372*, 346−348.
(7) Reyes, P.; Concha, I.; König, M. E.; Fierro, J. L. G. *Appl. Catal. A* **1993**, *103*, 5−16.
(8) Mojet, B. L.; Miller, J. T.; Ramaker, D. E.; Koningsberger, D. C. *J. Catal.* **1999**, *186*, 373.
(9) Koningsberger, D. C.; de Graaf, J.; Mojet, B. L.; Ramaker, D. E.; Miller, J. T. *Appl. Catal. A* **2000**, *191*, 205.
(10) Koningsberger, D. C.; Oudenhuijzen, M. K.; de Graaf, J.; van Bokhoven, J. A.; Ramaker, D. E. *J. Catalysis* **2003**, *216*, 178.
(11) Bond, G. C. *Catal. Today* **1993**, *17*, 399.
(12) Gault, F. G. *Adv. Catal.* **1981**, *30*.
(13) Foger, K.; Anderson, J. R. *J. Catal.* **1978**, *54*, 318−335.
(14) Zhang, Z.; Wong, T. T.; Sachtler, W. H. M. *J. Catal.* **1991**, *128*, 13−22.
(15) Larsen, G.; Haller, G. L. *Catal. Lett.* **1989**, *3*, 103−110.
(16) Ferrari, A. M.; Pacchioni, G. *J. Phys. Chem.* **1996**, *100*, 9032−9037.
(17) Jansen, A. P. J.; van Santen, R. A. *J. Chem. Phys.* **1990**, *94*, 6764.
(18) Ramaker, D. E.; de Graaf, J.; van Veen, J. A. R.; Koningsberger, D. C. *J. Catal.* **2001**, *203*, 7.
(19) López, N. *J. Chem. Phys.* **2001**, *114*, 2355−2361.
(20) Kua, J.; Goddard, W. A. *J. Phys Chem. B.* **1998**, 102 (47), 9481−9491
(21) Ramaker, D. E.; Oudenhuijzen, M. K.; Koningsberger, D. C. *Phys. Rev. B*, submitted.
(22) Oudenhuijzen, M. K.; van Bokhoven, J. A.; Miller, J. T.; Ramaker, D. E.; Koningsberger, D. C. *J. Am. Chem. Soc.*, in press, 2004.
(23) Ramaker, D. E.; Teliska, M.; Zhang, Y.; Stakheev, A. Yu.; Koningsberger, D. C. *Phys. Chem. Chem. Phys.* **2003**, *5*, 4492−4501.
(24) Teliska, M.; O'Grady, W. E.; Ramaker, D. E. *J. Phys. Chem. B* **2004**, *108*, 2333.
(25) Teliska, M.; O'Grady, W. E.; Ramaker, D. E. To be submitted.
(26) Kua, J.; Faglioni, F.; Goddard, W. A., III. *J. Am. Chem. Soc.* **2000**, *122*, 2309−2321.
(27) Kua, J.; Goddard, W. A., III. *J. Phys. Chem. B* **1998**, *102*, 9492−9500.
(28) Papoian, G.; Nørskov, J. K.; Hoffmann, R. *J. Am. Chem. Soc.* **2000**, *122*, 4129−4144.
(29) Amsterdam Density Functional Package ADF 2000.02, Department of Theoretical Chemistry, Vrije Universiteit, Amsterdam. http://www.scm.com.
(30) Becke, A. D. *J. Chem. Phys.* **1986**, *85*, 7184−7187.
(31) Perdew, J. P. *Phys. Rev. B* **1986**, *33*, 8822−8824.
(32) Philipsen, P. H. T.; van Lenthe, E.; Snijders, J. G.; Baerends, E. J. *Phys. Rev. B* **1997**, *56*, 13556.
(33) van Lenthe, E.; Baerends, E. J.; Snijders, J. G. *J. Chem. Phys.* **1994**, *101*, 9783.
(34) Olsen, R. A.; Kroes, G. J.; Baerends, E. J. *J. Chem. Phys.* **1999**, *111*, 11155−11163.
(35) Baerends, E. J.; Branchadell, V.; Sodupe, M. *Chem. Phys. Lett*, **1997**, *265*, 481−489.
(36) Yang, L.; DePristo, A. E. *J. Catal.* **1994**, *149*, 223−228.
(37) Renouprez, A.; Jobic, H. *J. Catal.* **1988**, *113*, 509−516.
(38) Davis, S. M.; Somorjai, G. A. *Surf. Sci.* **1980**, *91*, 73−91.
(39) Ko, C. S.; Gorte, R. J. *Surf. Sci.* **1985**, *161*, 597−607.
(40) Christmann, K.; Ertl, G. *Surf. Sci.*, **1976**, *60*, 365−384.
(41) Wang, H.; Tobin, R. G.; Lambert, D. K.; Fisher, G. B.; Dimaggio, C. L. *Surf. Sci.* **1995**, *330*, 173−181.
(42) Wang, H.; Tobin, R. G.; Lambert, D. K. *J. Chem. Phys.* **1994**, *101*, 4277−4285.
(43) Tsuchiya, S.; Amenomiya, Y.; Cvetanovic, R. J. *J. Catal.* **1970**, *19*, 245−255.
(44) Atkins, P. W. *Physical Chemistry*; W. H. Freeman: New York, 1986; p 817.
(45) Perry, J. K.; Tahir-Kheli, J.; Goddard, W. A., III. *Phys. Rev. B* **2001**, *63*, 144510.
(46) Paul, J. F.; Sautet, P. *J. Phys. Chem. B* **1998**, *102*, 1578−1585.
(47) Ruban, A.; Hammer, B.; Stoltze, P.; Skriver, H. L.; Nørskov, J. K. *J. Mol. Catal. A* **1997**, *115*, 421−429.
(48) Koper, M. T. M.; van Santen, R. A. *J. Electroanal. Chem.* **1999**, *472*, 126.
(49) Gasteiger, H. A.; Markovic, N.; Ross, Jr. P. N.; Cairns, E. J. *J. Phys. Chem.* **1993**, *97*, 12020.
(50) Rice, C. L. C.; Masel, R. I.; Babu, P. K.; Waszczuk, P.; Kim, H. S.; Oldfield, E.; Wieckowski, A. *J. Phys. Chem. B* **2002**, *106*, 9581.
(51) Lu, C.; Masel, R. I. *J. Phys. Chem. B* **2001**, *105*, 9793.